The International Journal of Advanced Manufacturing Technology (2018) 98:617–627
https://doi.org/10.1007/s00170-018-2245-x

ORIGINAL ARTICLE

Surface integrity assessment of M3 HSS cutting taps after grinding at various machining conditions

Saimon Vendrame[1] · Rosemar Batista da Silva[2] · Álisson Rocha Machado[2,3] · Eduardo Carlos Bianchi[1] · Paulo Roberto Aguiar[1] · Fabrício Guimarães Baptista[2] · Luiz Eduardo de Angelo Sanchez[1] · Mark J. Jackson[4]

Received: 9 October 2017 / Accepted: 30 May 2018 / Published online: 14 June 2018

Abstract
Grinding is a machining process that provides a combination of good surface finishing and tight dimensional tolerances on a machined component. Owing to these characteristics, it is employed in the finishing process of hardened parts, such as high-speed steel (HSS) cutting tools (principally drills and taps). Despite the various benefits, the specific energy in grinding is very high, resulting in high heat generated in the wheel–workpiece interface that could lead to thermal damages. To avoid such problems, aiming to maximize productivity and preserve the integrity of the machined component, a cutting fluid and cutting parameters must be properly selected. However, since the process dynamics is particular for each grinding process, especially in complex geometries, specific studies in real manufacturing conditions are required to understand the phenomena and minimize surface damages. In this context, this work aims to evaluate the surface integrity of M3 HSS cutting taps after they have been ground at various cutting conditions. Machining tests were performed in situ under controlled and variable wheel speed, depth of cut, and workpiece speed conditions. Machined surface images and microhardness below the surface were the output variables investigated. Results showed that, on average, the thickness of the affected surface layer was about 70% lower after machining at the lowest workpiece speed used. The correlation between grinding removal rates and thermal damage was also discussed.

Keywords Grinding · Surface integrity · Thermal damage · HSS

1 Introduction

There are several types of grinding processes with specific geometries and parameters. This diversity of processes enables the application of grinding in the manufacture of parts with different geometries such as ball bearings, automotive engine, and even turbine axles. Peripheral and cylindrical are the most common types of grinding and their cinematics are known and

✉ Saimon Vendrame
saimon.vend@gmail.com

Rosemar Batista da Silva
rosemar.silva@ufu.br

Álisson Rocha Machado
alisson.rocha@pucpr.br

Eduardo Carlos Bianchi
bianchi@feb.unesp.br

Paulo Roberto Aguiar
aguiarpr@feb.unesp.br

Fabrício Guimarães Baptista
fabriciogb@feb.unesp.br

Luiz Eduardo de Angelo Sanchez
sanchez@feb.unesp.br

Mark J. Jackson
mjjackson@ksu.edu

[1] Department of Mechanical Engineering, São Paulo State University "Júlio de Mesquita Filho", Bauru Campus, Av.Eng. Luiz Edmundo C. Coube, 14-01 – Vargem Limpa, Bauru, Sao Paulo 17033-360, Brazil

[2] School of Mechanical Engineering, Joao Naves de Ávila Avenue, Federal University of Uberlândia - UFU, 2121 – Campus Santa Monica, Uberlândia, Minas Gerais 38408-100, Brazil

[3] Mechanical Engineering Graduate Program, Pontifícia Universidade Católica do Paraná – PUC-PR, Curitiba, Praia 80215-901, Brazil

[4] Kansas State University, Polytechnic Campus, 2310 - Centennial Road, Salina, KS 67401-8196, USA

described by mathematical models [1–3]. Schumann et al. [1] used a finite element method (FEM) to describe a model of thermal load distribution into grinding zone providing a more accurate estimate, evidencing that there are great differences between flat and cylindrical grinding, and thus not always can the same heat source models be adopted. Barrenetxea et al. [2] showed, through simulations on grinding operation, that the tangential force and the specific energy per grit can be controlled through different strategies. Also, they reported that the proper selection of the work speed and infeed rate in a controlled kinematics way can reduce the risk of burning.

The heat transfer in grinding must be approached from two points of view: the global effect that considers the grinding wheel interaction and grinding parameters, and the local effect, which takes into account the effect that each grain offers when removing material. Hou and Komanduri [3] described and compared different heat source models considering the local heat effect of multiple grains.

There are also some specific grinding processes in which path and cinematics are peculiar and more difficult to be described [4, 5]. The work carried out by Ren et al. [4], for instance, described the movements of the workpiece and the grinding wheel in flute grinding, so it was possible to determine more precise parameters for the manufacture of milling cutters. In other research, Drazumeric et al. [5] carried out the kinematic analysis of the grinding of a non-round workpiece and through a thermal model showed the importance of estimation of the contact region between tool and workpiece.

The grinding process of cutting taps can be classified as external cylindrical profile grinding and is an example of complex geometry.

Because of the many aspects involved, grinding is one of the most complex conventional machining processes. In technological applications, over the traditional requirements, such as low surface roughness and tight dimensional tolerances, the control of the subsurface properties such as residual stress distribution and acceptable microhardness variation in the microstructure is required. Thus, the assurance of surface and subsurface integrity plays an important role in grinding [6]. There are four groups of variables that can affect the surface integrity of ground parts as follows [7]:

(a) Grinding machine: stiffness, accuracy, stability, vibration, and thermal deflections;
(b) Grinding wheel: abrasive grain size, material properties, structure, porosity, hardness, and binder;
(c) Workpiece material properties: yield stress, fracture toughness, and phase transformation temperature;
(d) Grinding parameters: cutting speed, workpiece speed, depth of cut, coolant, and dressing conditions.

Among the several types of defects associated with the heat generated during grinding that can be encountered on the surface and subsurface of a ground part, the most common ones are phase precipitation, softening, phase transformations leading to rehardening, cracking, residual stress, and chemical reactions (associated with burn marks) [7].

Severe burn marks are easily recognized visually in such cases by the appearance of dark blue stripes. This damage is generally associated to low workpiece speed and can be avoid if the speed is increased. In many cases, burn is not so readily recognized because burn marks may have been removed in the final spark-out period of grinding. However, if the burn is deep enough, the removal of the external evidence of burn will not be sufficient to eliminate other aspects of damage such as modified hardness or even cracks extending below the surface [8].

Thermal damages can be usually avoided or overcome by the correct selection of grinding conditions in one of the following ways: redressing the grinding wheel to produce a sharper cutting surface; replacing the grinding wheel with a softer grade or more open structure; replacing the grinding wheel with a sharp superabrasive; improving fluid delivery or changing the grinding fluid; or reducing removal rates [8]. Grinding parameters can change the dynamic contact area between the wheel and the workpiece.

During the process, the contact area between the abrasive grits of the wheel and the workpiece is very small compared to that for conventional machining process with defined cutting edges of the tool, like milling, for instance. The importance of such contact area is because of its direct relationship with the undesirable thermal effects of the process caused by excessive heat being transferred to the workpiece during machining [9, 10], particularly with conventional abrasive wheels that have poor thermal conductivity.

Several mathematical models have been developed to study the relation between grinding parameters and cutting temperatures. Some models proposed [11–15] have shown that energy partition into wheel or workpiece is mainly governed by the characteristics of the pair of wheel–workpiece materials. These works have demonstrated that the specific grinding energy (the amount of energy spent per unit of removed material) is dependent not only on the grinding process parameters, but also on the physical–mechanical properties of the workpiece material. Each one of these cited works [11–15] is discussed individually below.

Lavine and Jen [11] used temperature models in the grinding zone to predict occurrence of film boiling and its consequence in damage to the workpiece (steel). Through the results, the authors highlighted mainly the difference between the abrasives used. When using the CBN wheel, there was no occurrence of burn even in the presence of the film boiling, unlike when machining with the aluminum oxide grinding wheel, that caused thermal damages on the workpiece.

Shaw [12] used a calorimeter method to measure the heat generated in finish grinding with aluminum oxide grinding

wheel and reported all the heat generated in grinding is converted to heat about 80% of which flows to the part. In addition, this author concluded that while the cutting speed plays a relatively small influence on specific energy, undeformed chip thickness has the highest influence. Although this was a very important study, it did not take into account the material influence.

Mayer et al. [13] using previously developed mathematical correlations showed the threshold among the parameters responsible for the burning occurrence. They described that critical grinding temperature can be expressed in terms of specific grinding energy input; however, it is necessary to know the values of the two material coefficients also involved in the grinding burn expression which depend on the particular workpiece material, its thermal properties, and the critical temperature. Although there are deviations, such model was very representative and had a satisfactory accuracy in predicting thermal damage through the parameters tested.

In another work carried out by Zarudi and Zhang [14], the authors showed that grinding parameters can shift the heat distribution and the heat source leading to an unstable condition and, consequently, resulting in the worst results in relation to the thermally affected layer. In addition, this work points out that the depth of cut is the parameter that causes less influence on the energy partition, and that partition is governed mainly by the materials of the workpiece and the grinding wheel.

Ren et al. [15] carried out a study on determination of specific energy in grinding of tungsten carbides with different grain sizes and found that cutting parameters and physical–mechanical and thermal properties of the workpiece materials must be taken into account in the analysis. Under the same machining conditions, materials with the same composition but different microstructures resulted in different specific energies. This occurs because the chip removal mechanisms are modified.

Malkin [16] has developed a work in which are shown several temperature models. According to the author, there are many factors that have to be considered in a thermal analysis, such as the contact area between the grinding wheel and the workpiece, the energy partition, and the temperature limit for the thermal damage occurrence. Furthermore, these factors have to be related with the grinding parameters and the properties of the workpiece materials. That shows that the thermal analysis strongly depends on each system wheel–workpiece environment and the machining parameters employed.

Another factor observed in the grinding is the formation of burr near the edges. When machining with circular paths as in top milling, burrs can be formed and are dependent on the cutting edge trajectory and workpiece geometry [17]. Although there are many differences between these processes, from a chip formation generation perspective and at lower depth of cut values in milling, grinding can be very similar to milling. So, comparing both processes in the same proportion of the depth of cut, the grinding burrs have a considerable size. Avila and Dornfied [18] showed that the input and output geometries of tool engagement are more related to burr than the machining parameters. In addition, they investigated different strategies so that they could be avoided. It is important to highlight that the deburring process is an additional operation that increases the cost of the manufactured product.

Tap manufacturing is a peculiar and complex machining process due to its geometry. Furthermore, taps are tools that need to be of very high qualities in terms of dimensions, surface, and subsurfaces. Owing to the scarce literature about grinding of taps, this work aims to contribute to machining users with important information obtained after grinding of the high-speed steel (HSS) cutting taps under various cutting conditions.

2 Experimental procedure

Experimental tests were carried out under real machining conditions in situ in a line production of a renowned cutting tool manufacturing company in Brazil. The process was performed in a five-axis CNC grinding machine in which the grinding wheel moves in a longitudinal tangential path in the direction of the workpiece. As shown in Fig. 1, the part previous the machining already has the helical flutes in a region with stock removal where the tap threads will be formed. The grinding wheel moves forward (Fig. 1a) without contact with the workpiece as it rotates. The displacement forward that the grinding wheel performs is the depth of cut (a_e). The number of steps required is set automatically through CNC programming. Depending on the amount of stock removal, depth of cut values employed can be varied until the final dimensions of the workpiece are reached. The workpiece speed can also vary between the roughing and finishing passes. After the grinding wheel advances, the workpiece moves parallel to the grinding

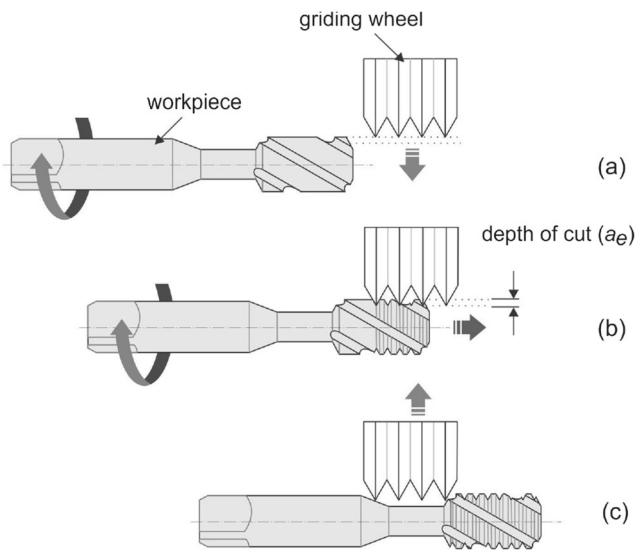

Fig. 1 Representation of the process of threading grinding of taps

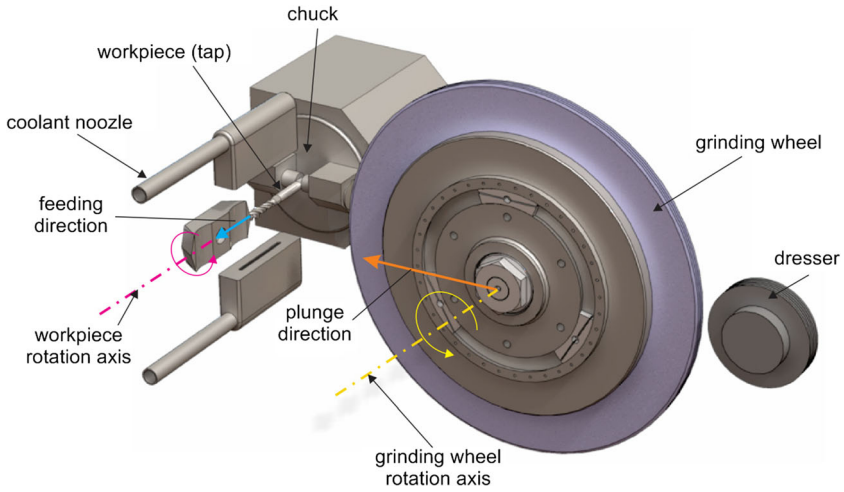

Fig. 2 Schematic view of the setup of the grinding operation of taps

wheel axis and towards it (Fig. 1b). The feed rate (longitudinal feed speed) is synchronized with its rotation so that threads are formed with the correct pitch. Thus, what defines this longitudinal feed rate is the workpiece speed. So, after the grinding wheel passes over the region with stock removal, the movement of the workpiece stops and the grinding wheel moves away, as illustrated in Fig. 1c. After each grinding pass, the grinding wheel is dressed with a rotary dresser. For each cutter geometry, there is a specific dresser with the desired grinding wheel profile, which defines the geometry of the machined threads. The workpiece moves to its initial position and the process repeats again from the first step, as illustrated in Fig. 1a. The process is completed upon reaching a sufficient number of passes to generate the threads of the desired size.

The grinding tests were performed by the experimental setup presented in Fig. 2**.** The workpiece is clamped by a chuck and coupled to a tail stock, avoiding deflections and vibration. Coolant nozzles are positioned at the top and bottom of workpiece axes and simultaneously actioned during the grinding operation. A mineral-based neat oil was employed as coolant in all the tests conditions, delivered by the flooding mode. The grinding wheel is a 320-mesh aluminum oxide grinding wheel with designation CS33A320HH4VB1. The wheel has the profile of the threads to be grinded. In order to provide this geometry to the grinding wheel, a diamond rotary dresser is positioned at the opposite side of the workpiece. After every pass of the abrasive wheel in a radial direction into the workpiece to generate threads (rear and front flank faces), the grinding wheel was dressed with 30 μm.

The tap material is AISI M3–high-speed steel grade with the following chemical composition: 1.21% C; 4.25% Cr; 5.0% Mo; 6.0% W; 3.0% V. The main characteristic of this steel grade is the considerable level of vanadium (at least 3%). The taps have 1/4″ (6.35 mm) diameter and three helical flutes (with approximately 45° of helix angle).

In order to investigate the effect of the machining parameters on the output variables analyzed in this work, three main input parameters were tested: cutting speed (v_c), work table speed (v_w), and depth of cut (a_e). The experimental matrix adopted was the full factorial 2^4 at two levels, which is presented in Table 1. The levels were defined based on preliminary tests and in accordance with the values employed in the cutting tap manufacturing industry.

After the machining tests, the taps were sectioned and their threads (produced by grinding) were taken to be examined with an OLYMPUS Evolution Color optical microscope, model SZ6145TR, having a digital camera in which the pictures are analyzed via an Image Pro-Express 5.1 software. After capturing the images from the threads, the specimens were cut and a single thread (composed by rear (trailing) and front (leading) flank faces) was detached from each specimen as shown in Fig. 3a. So, the detached thread was embedded in an acrylic resin together with a part of the same material in order to avoid rounding of edges during the sanding polishing operations. Silicon carbide sandpapers in the sequence of 80, 120, 320, and 400 mesh were initially used. Then, diamond polish pads with 600 and 1200 mesh grades (Aka-Piato model by Akasteel) were used. Diamond pads were used due to the higher hardness of M3-HSS material (65HRc).

Table 1 Machining conditions of the grinding tests

test condition	Cutting speed (v_c [m/s])	Work speed (v_w [m/min])	Depth of cut (a_e [mm])
C1	(−) 50	(+) 13.0	(−) 0.02
C2	(+) 80	(+) 13.0	(−) 0.02
C3	(−) 50	(−) 4.0	(−) 0.02
C4	(+) 80	(−) 4.0	(−) 0.02
C5	(−) 50	(+) 13.0	(+) 0.03
C6	(+) 80	(+) 13.0	(+) 0.03
C7	(−) 50	(−) 4.0	(+) 0.03
C8	(+) 80	(−) 4.0	(+) 0.03

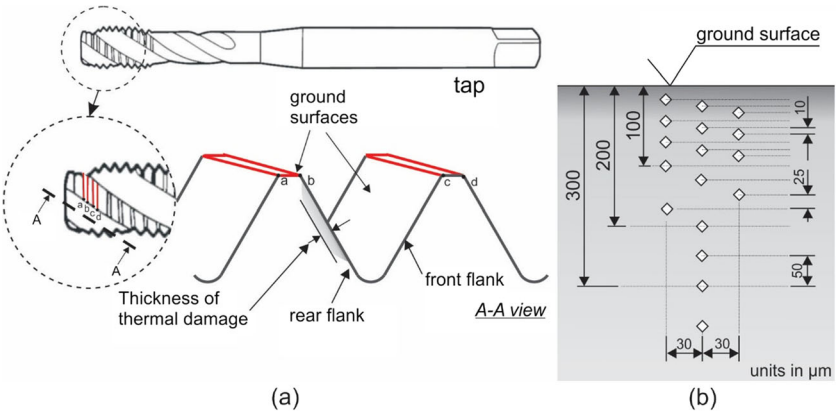

Fig. 3 Region of occurrence of burr and thermal damage. **a** Schematic view of selection of the ground surfaces analyzed and measurement of thickness of thermal damage. **b** Details of microhardness test methodology: distance between indentations during measurement of microhardness

The microhardness measurements were done using a SHIMADZU microhardness tester HMV-2 series with a 0.98 kgf of loading (9.6 N (HV0.1)) for 15 s. The measurements started from a depth of 10 μm below the machined surface and were taken up to 100 μm, keeping the intervals of 20 and 30 μm in the vertical and horizontal directions, respectively, as shown in Fig. 3b. From 100 to 200 μm below the machined surface, measurements were taken in intervals of 25 μm, and after that at 50 μm each.

3 Experimental results and discussion

As a first approach, a visual inspection was carried out in order to investigate regions with occurrence of burn marks and burrs. In Fig. 4a, b, the images of the tap threads are shown after the grinding process. From Fig. 4a, the presence of burr in the rear flank of the ground surface of the tap as well as the evidence oxide mark on the flute surface near the rear flank can be seen. It can be noticed that the mark occurs only at one side, preferentially in the rear flank of the thread. The presence of a darkened oxide mark is the evidence that higher temperatures were reached in this region. Burrs are undesirable protrusions formed on the machined surface, generally in the lateral edge of the workpiece as results of the plastic deformation deriving from cutting processes [18], and they must be removed by a deburring process. However, the deburring process is an additional operation that increases the cost of the manufactured product.

In all the conditions tested, it was observed the presence of burrs and oxide marks, and in some cases, the marks, is more darkened and thicker. Thus, using the optical microscope, images of taps were inspected. Analysis was made of the rear flank: once on that region, they had the most evident burning marks, and, with the post-processor image software, measurements were made of the thickness of each burn mark.

In Fig. 5a–f, the threads of tap images after machining under different cutting conditions are shown (Table 1). From the darkened marks, it can be inferred that intense heat was generated during machining. The machining conditions, C3 and C1 (Table 1), are related to the grinding conditions with lower cutting speed and depth of cut. After comparing images of threads machined under C3 and C1 conditions, it is possible to note that the oxide mark in the lateral edge of the thread obtained after C3 condition (Fig. 5a) is larger than that in the image under the C1 condition (Fig. 5b), at the highest work speed (Table 1), thereby indicating that dark burn marks in thread flanks were more visible when machining under low work speed.

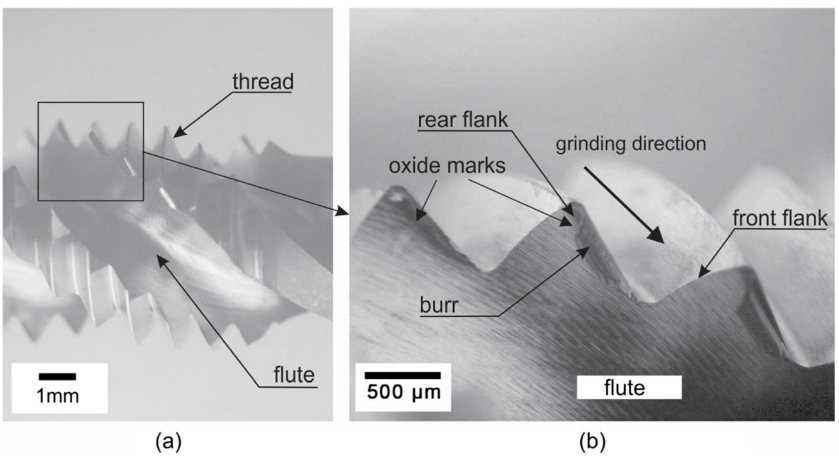

Fig. 4 **a** Image of the tap threads after grinding operation. **b** Close view of the depicted region, showing burrs and oxide marks

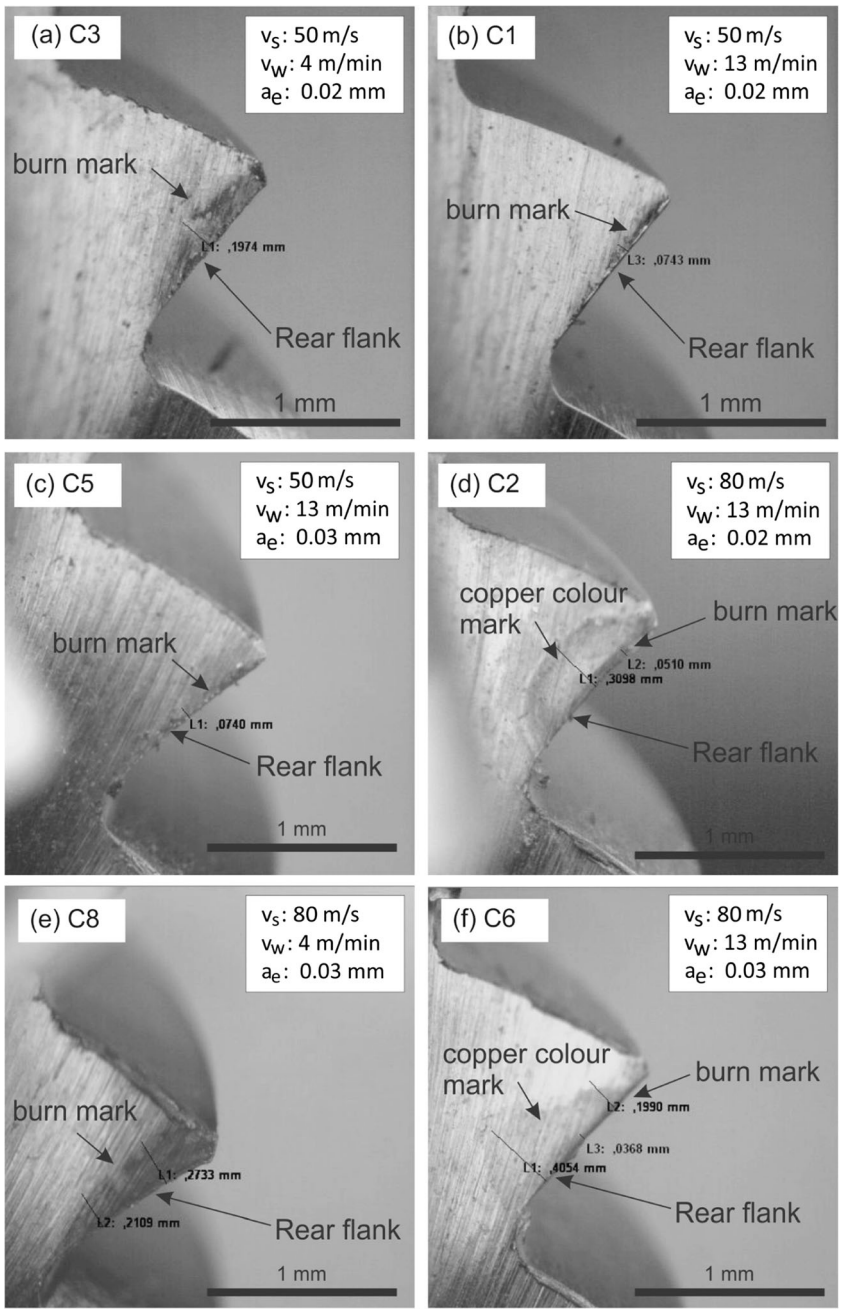

Fig. 5 Threads of taps showing darkened marks due to the grinding process under the following machining conditions: **a**, **b** machining conditions at low wheel speed; **c**, **d** intermediate conditions; and **e**, **f** condition with high wheel speed level

As shown in Table 1, from C1 to C5 conditions, the depth of cut was increased, whereas from C1 to C2 conditions, the increase was in the cutting speed. Comparing the burn marks in rear flank at C1 (Fig. 5b) with the marks of condition C5 (Fig. 5c), it is not possible to distinguish the difference between them. However, comparing the images of rear flank of taps machined under C1 (Fig. 5b) with C2 (Fig. 5d) conditions, it is possible to observe that a copper-colored mark around a black band near the edge of the tap machined under C2 condition is evident (this copper color is not seen because the images are in black and white). This can be an indication that the cutting speed changed the heat distribution partition in that rear flank thread. Nevertheless, the copper color does not represent a microstructural change, as will be shown forthcoming.

Images of the tap threads machined with C8 and C6 conditions are shown in Fig. 5e, f, respectively, and they are the conditions with high cutting speed values. The regions in the rear flank of the threads machined under C8 conditions are darker than those obtained after machining under C6 condition, despite both being produced at the highest work speed level. The difference between groups of low level and high level of machining conditions is the cutting speed. From the images of different groups, it can be demonstrated for this geometry that

Table 2 Measurement results of burn marks in rear flank of cutting tap threads

Machining conditions	Burn mark thickness [mm]		Mean [mm]	Mean standard deviation [mm]
	Replica			
	A	B		
C1	0.074	0.073	0.073	0.001
C2	0.309	0.289	0.299	0.014
C3	0.197	0.256	0.227	0.041
C4	0.220	0.240	0.230	0.014
C5	0.074	0.078	0.076	0.003
C6	0.405	0.429	0.417	0.016
C7	0.219	0.217	0.218	0.001
C8	0.260	0.270	0.265	0.007

the increase in the work speed is beneficial for the process, regardless of the cutting speed used, as expected [7].

From the images of tap threads, it was possible to measure the thickness of the darkened marks close to the rear flank. In all conditions, the same measurement criterion was adopted. In Table 2, the results for all the test conditions, from C1 to C8 and for the two replicates ones, A and B, are shown.

To obtain statistical support and confirm these relationships, a statistical analysis was performed using the analysis of variance (ANOVA) test. This test helps in the identification of the statistical influence of each parameter and their interactions in the experimental results.

From the results presented in Table 3, the p value is lower than 0.05 for the workpiece speed (v_w), indicating that there is statistical significance regarding the parameter and that affects the thickness of the burn marks, unlike for the other parameters and their interactions, since the p values are above the significance reference. Since the interactions are not significant, a new analysis was performed considering only the main parameters and excluding the interactions. The result is presented in Table 4.

The result shown in Table 4 indicates that, even disregarding the first-order interactions, the effect of the work speed parameter plays significant influence in relation to the thickness of the burning mark measured.

Table 3 ANOVA test results

Parameter	Df	Sum Sq	Mean Sq	F value	Pr (> F)
v_w	1	55,995	55,995	226.215	0.0423*
a_e	1	104	104	0.419	0.6343
v_s	1	63	63	0.253	0.7031
v_w:a_e	1	62	62	0.251	0.7043
v_w:v_s	1	790	790	3.192	0.3249
a_e:v_s	1	218	218	0.882	0.5199
Residuals	1	248	248		

*Statistically significant

Table 4 ANOVA results excluding first-order interactions

Parameter	Df	Sum Sq	Mean Sq	F value	Pr (> F)
v_w	1	55,995	55,995	169.924	0.0002*
a_e	1	104	104	0.315	0.6048
v_s	1	63	63	0.19	0.6852
Residuals	4	1318	330		

*Statistically significant

Visual inspection of the workpiece surface may be useful to qualitatively detect some subsurface changes resulting from a grinding process in which the machining conditions were unappropriated selected. However, the marks do not often represent a microstructural alteration and can be confused with oxidation present in a thin layer on the surface. Thus, in order to confirm the microstructural change associated with the dark burn marks observed, microhardness measurements were made near the thread flanks.

In Fig. 6a, b, the results of microhardness measurements in the specimens ground under the lowest cutting speed value of 50 m/s (C3 and C7 conditions) are shown, but with different work speed values. These conditions are related to the group of low level of cutting speed parameters. In general, microhardness values next to the machined surface were lower than the average of hardness measured prior to grinding operation, regardless of the work speed tested. Machining under the condition C3, Fig. 6a caused alteration in microhardness in up to 50 μm below the machined surface, while for the C7 condition (Fig. 6b), where work speed is higher than C3 condition, such microhardness alteration occurred nearly to 25 μm.

Figure 7a, b shows the microhardness results for the workpiece samples after machining under intermediate C5 and C8 conditions. When comparing condition C8 (Fig. 7b) with condition C5 (Fig. 7a), it can be observed that microhardness values were lower than the average of hardness measured prior to grinding operation at distances of up to 60 and 70 μm below the machined surface, respectively.

Figure 8a, b shows the microhardness values measured after the grinding of specimens under the more severe grinding conditions, C2 and C6. In both cases, a change in the microhardness is observed and for C2 the region extends to a distance over 100 μm from the machined surface, while for C6 condition the drop in hardness is kept up to 75 μm below the machined surface. The difference between these conditions is the work speed. It can be seen that the behavior for microhardness of workpieces machined with C2 and C6 is similar to that for conditions C3 and C7 (in Fig. 6a, b), which was employed at low levels of machining parameters. It was observed from this result that, for the lower workpiece speeds, the thickness of the affected layer is about 60% higher.

The results of the microhardness measurement showed that the higher levels of the work speed parameter (v_w) resulted in a

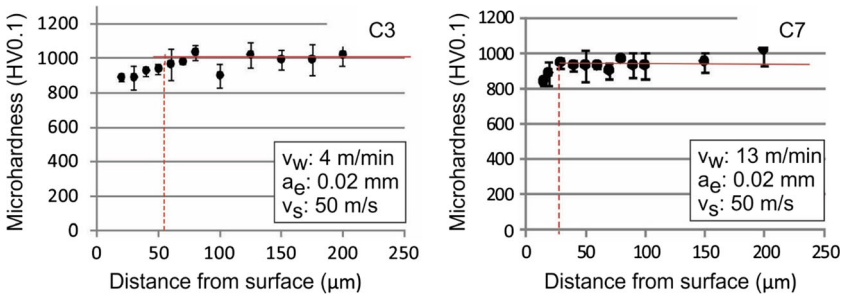

Fig. 6 Microhardness measurement results for the specimens ground under low level machining conditions **a** C3 and **b** C7

smaller thickness of microstructurally affected layer from the ground surface. For the parameters cutting speed (v_s) and depth of cut (a_e), they appear to not influence the thickness of the damaged layer. These results confirm those evidenced from visual inspection. Machining under C2 and C6 conditions provided machined surface having copper colors, even though such marks cannot represent a microstructural change, which this type of test was able to detect.

With exception of C2 and C6 conditions, overall results in Figs. 4, 5, and 6 showed that decrease in the microhardness near the ground surface is probably due to an overtempering caused by the concentrated heat in this region during the grinding process. No evidence of rehardening on the machined surfaces was observed, since no increase in hardness in regions near the machined surface was recorded under the conditions investigated. Also, from all the results obtained in this work, it is clear that there are several aspects regarding grinding burn, such as cooling-lubrication conditions, workpiece material, grinding wheel, and machining parameters. Since the cooling conditions and the material are not the focus of this work, the further discussion is based only on the machining parameters. There are some hypotheses that can be discussed as follows: (i) the increase of the cutting speed lead to a change of heat distribution in the cutting zone; (ii) low workpiece speed leads to a greater surface damage because of longer contact time between grinding wheel and workpiece material compared to high workpiece speed; (iii) decrease in the depth of cut leads to thermal damage due the increase of energy per unit of material removed. These are further discussed here.

(i)The increase of the cutting speed causes a change of heat distribution in the cutting zone Through the result analysis obtained in this work, it can be concluded that the cutting speed does not play significant influence on surface and subsurface damages. Comparing the pair of conditions with higher cutting speed, C4 and C6 with C2 and C3, respectively, it can be noted that they are very close in terms of thickness of thermal damaged layer. Although there were observed copper-colored marks near the rear flank of the taps ground under 80 m/s of cutting speed, C4 and C6 conditions, shown in Fig. 5d, f, respectively, it cannot be inferred that microstructural changes occurred based on the microhardness analysis.

It is known that, for regular shallow cut grinding with vitrified aluminum oxide wheels, the fraction of the grinding energy transported as heat to the workpiece at the grinding zone is typically 60–85% [12, 16]. Considering the heat flux from the grinding zone to the workpiece as being uniformly distributed, the amount of heat transferred depends mainly on the contact area and the velocity of this heat source [16]. Therefore, once the grinding wheel speed is increased, the heat source does not move from the grinding zone, and the workpiece speed, not the cutting speed, will be responsible for moving this source out. In some cases, the increase of cutting speed could result in a less efficient process due to the grinding wheel wear. The reason is that with the increase of the wheel speed, more abrasive grains rub against the workpiece material surface, increasing the heat generation and leading to more transference of heat to the workpiece [19]. On the other hand, under certain circumstances, if the wheel speed is increased enough, the temperatures would fall [9]. The phenomenon interpretation is that a heated surface facilitates the removal of the next chip and so reduces the grinding forces, also known as dynamic hardness. The rise of grinding wheel speed could cause expulsion of the cutting fluid from the cutting zone, which leads to the fluid boiling, thereby

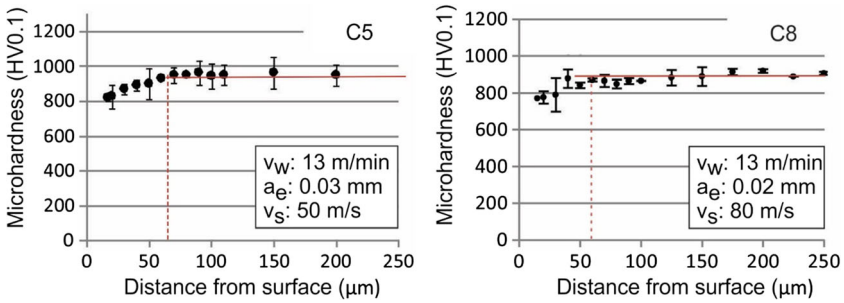

Fig. 7 Microhardness values after machining with the intermediate level machining conditions **a** C5 and **b** C8

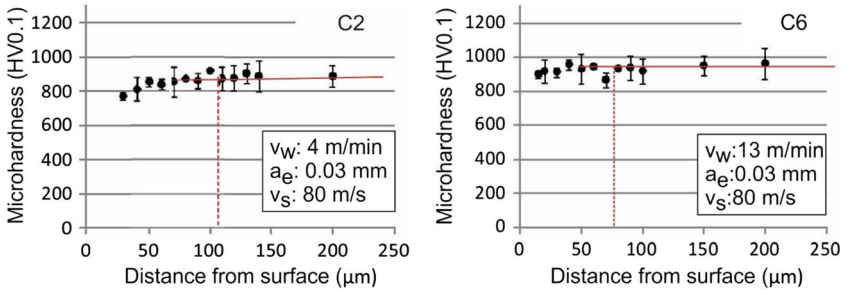

Fig. 8 Microhardness measurement results for the specimens ground under higher level machining conditions **a** C2 and **b** C6

reducing the coolant efficiency [11]. This may be the cause of the observed copper-colored marks near the flank (Fig. 5d, f); however, due to the complex geometry of the tap thread investigated in this work, it is difficult to confirm that statement. Although the cutting speed did not show great effect in the thermal damage results of this work, the increase of cutting speed is associated with the surface finish (roughness) on the ground surface of the cutting tap threads; in general, the increase of cutting speed results in a better finishing [19].

(ii)Low workpiece speed causes greater surface damage The workpiece speed played an important influence on the surface integrity of the workpiece material. Severe thermal damages were observed when machining at a lower work speed, 4 m/min, especially when combined with the higher depth of cut, $a_e = 0.03$ mm, C5 condition (Fig. 5e), and those were confirmed by the highest drop in hardness in regions very close to the machined surface (Fig. 8a), unlike those observed for the workpiece materials machined at higher workpiece speed. This can be attributed to the increased contact time between the grinding wheel and the workpiece material when machining at low workpiece speeds.

As previously reported, some thermal models in grinding [9–12, 16] proposed a uniform heat flux from the grinding zone to the workpiece. From these models, the cutting parameters could influence the heat generation or the heat flux intensity. The heat generation is mainly associated with the energy spent in the process of cutting, plowing, and sliding, phenomena always present in grinding [19]. Focused only in the heat flux, when the workpiece speed increases, the heat source above the surface is moved away. The result indicates an inverse relationship between thermal damage and workpiece speed, because when the workpiece speed is increased, less thermal damage or a thinner layer of microstructural change is observed [11]. In fact, various empirical models obtained from experimental results, such as that proposed by Mayer et al. [13], describe a threshold to burn avoidance. These models depend on the abrasive and the work material, besides the machining conditions, but in general the burns were observed in low workpiece speeds and high material removal rates.

(iii)Decrease in the depth of cut leads to thermal damage Figure 9 shows the test machining conditions arranged in decreasing order of equivalent chip thickness and the thermal damage thickness measured. At the same time that C1 and C5 conditions are those with the highest thermally affected layer, they are also the ones with the lowest equivalent chip thicknesses. According to Malkin and Guo [19], an increase in cutting speed affects the equivalent chip thickness (Eq. 1), i.e., it reduces the chip thickness. This effect, however, can be overcome by increasing the friction between flattened abrasive grains and the workpiece material surface. The energy used to remove material can be decreased, but the energy of slip friction increases and the result will depend on the balance of them.

$$h_{eq} = a_e . \frac{v_w}{v_c} \tag{1}$$

Where a is the radial depth of cut, v_c is the cutting speed, and v_w is the work speed.

Furthermore, according to Malkin and Guo [19], the specific energy decreases as the material removal rate increases, in this case by the increase in workpiece speed, thereby leading to increase in the fraction of the heat remaining in the grinding path and consequently reduction of the depth of the thermally affected layer, which results in shallower heat penetration and shorter heating times.

Even though the material removal rate was increased with the depth of cut, by comparing the low and high levels of cutting conditions with the intermediate conditions, no significant difference was observed. Although the specific literature [3, 16] appoints that the heat generated is higher for high

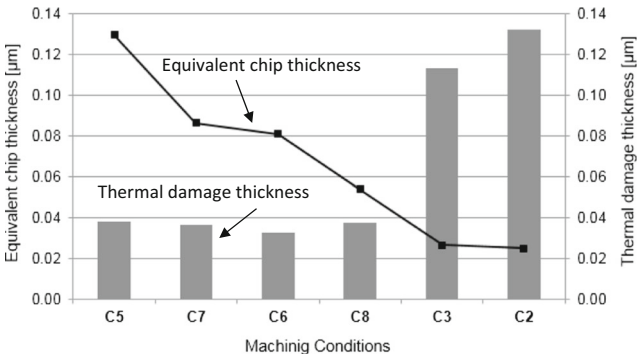

Fig. 9 Calculated equivalent chip thickness and thermal damage layer thickness for each machining condition in Table 1

removal rates, in this case, the range of the parameters selected did not affect the thickness of thermal damaged layer. Among the machining conditions investigated in this work, those in which the highest work speed was employed showed to be the suitable ones for grinding M3 HSS cutting taps in terms of thermal damage layer. It is important to note that the cutting speed should be chosen in an intermediate condition respecting the surface finish and the dimensional tolerances.

The presence of thermal damage on the flanks of the taps is directly related to their wear resistance. Soderberg and Hogmark [20] conducted tests on different machining processes and reported that abrasive wear is the predominant wear mechanism in high-speed steel tools. The amount and distribution of the primary carbides are the main factors that increase the resistance to wear because they act as a barrier to abrasive particles of the grits of the grinding wheel. On the other hand, the hardness of the matrix has a fundamental role in giving the support to these carbides and preventing them from being pulled out. Chaus and Hudáková [21] evaluated the abrasive wear performance of cast and rolled high-speed steels and demonstrated that the carbide distribution plays a key role in abrasive wear resistance. Moore [22] complements that high-speed steel microstructure has a fundamental role in the resistance to wear and that is a linear relationship between abrasive wear resistance and bulk hardness.

Arul Saravanapriyan et al. [23] carried out turning tests using coated and uncoated tools with and without grinding burn marks, in which for the latter the affected layer was about 200 μm and with the presence of a small hardened region near the surface. The authors found that the material near the tool flank does not provide sufficient anchoring for the coating, so leading to a flaking of the coating and reducing the tool life.

Due to the rotation of the workpiece, a grinding wheel entry always occurs in an edge between the thread and the flute. This type of grinding has a characteristic of interrupted cutting owing to a presence of the flutes of the cutting taps. As shown in this work, the main thermal damages found are on the threads, near the rear flanks, where the grinding wheel penetrates and leaves the workpiece. Further studies to better assess the subsurface alterations on the HSS tools caused by the variation of the input parameters tested are needed, such as tensile testing and X-Ray diffraction to measure tensile strength, ductility, and residual stresses of machined components.

4 Conclusions

From the results obtained from in situ experimental tests in grinding of M3 HSS cutting taps, the following conclusions can be drawn:

- The presence of burrs and oxide marks was observed in most of the cutting tap threads.
- Grinding burn marks near the tap thread were more pronounced after machining with the lowest work speed ($v_w = 4$ m/min). Grinding burn is a general indication of microstructural changes as a result of heat generated during grinding operation. Under the lowest work speed, the highest microhardness variation below the machined surface was also observed. It was found that, after performing the ANOVA test, the work speed parameter played a significant influence on the thickness of the burning mark measured.
- The cutting speed did not play a significant influence on the microhardness changes and in the thermal damage layer below the machined surface.
- Grinding at the combination of the highest cutting and work speed values and the lowest depth of cut parameters (C2 condition) generated copper-colored marks around a black band near the edge of the tap machined, meaning that the cutting speed changed the heat distribution partition in the tool flank.
- Increase in the depth of cut caused a higher thickness of the thermal damage layers, except when machining with the lowest cutting speed of 50 m/s.
- No evidence of rehardening on the machined surfaces was observed in all the conditions tested.

Funding information Two of the authors thank the Post-Graduate Program in Mechanical Engineering of the Federal University of Uberlândia, CAPES-Proex, and CNPq for the financial support. One of the authors thanks FAPEMIG for the financial support received through PPM-VII Project, Process No. PPM-00265-13 as well as the CAPES for the financial support given by a PNDP project—post-doctoral scholarship at the Post-Graduate Program of Electrical Engineering of FEB-UNESP-BAURU (2016–2017).

References

1. Schumann S, Siebrecht T, Kersting P, Biermann D, Holtermann R, Menzel A (2015) Determination of the thermal load distribution in internal traverse grinding using a geometric-kinematic simulation. Procedia CIRP 31:322–327. https://doi.org/10.1016/j.procir.2015.03.020
2. Barrenetxea D, Alvarez J, Marquinez JI, Sanchez JA (2016) Grinding with controlled kinematics and chip removal. CIRP Ann. - Manuf. Technol. 65:341–344. https://doi.org/10.1016/j.cirp.2016.04.097
3. Hou ZB, Komanduri R (2004) On the mechanics of the grinding process, part II—thermal analysis of fine grinding. Int J Mach Tools Manuf 44:247–270. https://doi.org/10.1016/j.ijmachtools.2003.09.008
4. Ren L, Wang S, Yi L, Sun S (2016) An accurate method for five-axis flute grinding in cylindrical end-mills using standard 1V1/1A1 grinding wheels. Precis Eng 43:387–394. https://doi.org/10.1016/j.precisioneng.2015.09.002
5. Drazumeric R, Badger J, Krajnik P (2014) Geometric, kinematical and thermal analyses of non-round cylindrical grinding. J Mater

Process Technol 214:818–827. https://doi.org/10.1016/j.jmatprotec.2013.12.007
6. M.J. Jackson, J.P. Davim, Machining with abrasives, 2011. doi: https://doi.org/10.1007/978-1-4419-7302-3.
7. J.P. Davim, Surface integrity in machining, 2010. doi:https://doi.org/10.1007/978-1-84882-874-2.
8. W.B. Rowe, Principles of modern grinding technology: second edition, 2013. doi:https://doi.org/10.1016/C2013-0-06952-6.
9. I.D. Marinescu, W.B. Rowe, B. Dimitrov, H. Ohmori, I.D. Marinescu, W.B. Rowe, B. Dimitrov, H. Ohmori, 6—Thermal design of processes, in: Tribol. Abras. Mach. Process., 2013: pp. 137–184. doi:https://doi.org/10.1016/B978-1-4377-3467-6.00006-9.
10. Malkin S, Anderson RB (1974) Thermal aspects of grinding: part 1—energy partition. J Eng Ind 96:1177. https://doi.org/10.1115/1.3438492
11. Lavine AS, Jen T-C (1991) Coupled heat transfer to workpiece, wheel, and fluid in grinding, and the occurrence of workpiece burn. Int J Heat Mass Transf 34:983–992. https://doi.org/10.1016/0017-9310(91)90009-4
12. Shaw MC (1996) Energy conversion in cutting and grinding*. CIRP Ann. - Manuf. Technol. 45:101–104. https://doi.org/10.1016/S0007-8506(07)63025-X
13. Mayer JE, Price AH, Purushothaman GK, Dhayalan AK, Pepi MS (2002) Specific grinding energy causing thermal damage in helicopter gear steel. J Manuf Process 4:142–147. https://doi.org/10.1016/S1526-6125(02)70140-0
14. Zarudi I, Zhang LC (2002) A revisit to some wheel–workpiece interaction problems in surface grinding. Int J Mach Tools Manuf 42:905–913. https://doi.org/10.1016/S0890-6955(02)00024-X
15. Ren YH, Zhang B, Zhou ZX (2009) Specific energy in grinding of tungsten carbides of various grain sizes. CIRP Ann. - Manuf. Technol. 58:299–302. https://doi.org/10.1016/j.cirp.2009.03.026
16. Malkin S, Guo C (2007) Thermal analysis of grinding. CIRP Ann. - Manuf. Technol. 56:760–782. https://doi.org/10.1016/j.cirp.2007.10.005
17. Aurich JC, Sudermann H, Bil H (2005) Characterisation of burr formation in grinding and prospects for modelling. CIRP Ann - Manuf Technol 54:313–316. https://doi.org/10.1016/S0007-8506(07)60111-5
18. M.C. Avila, D.A. Dornfeld, On the face milling burr formation mechanisms and minimization strategies at high tool engagement, in: 7th Int. Conf. Deburring Edge Finish., 2004.
19. S. Malkin, C. Guo, Grinding technology: theory and applications of machining with abrasives, 2nd ed., Industrial press Inc., 2008.
20. Söderberg S, Hogmark S (1986) Wear mechanisms and tool life of high speed steels related to microstructure. Wear 110:315–329. https://doi.org/10.1016/0043-1648(86)90106-7
21. Chaus AS, Hudáková M (2009) Wear resistance of high-speed steels and cutting performance of tool related to structural factors. Wear 267:1051–1055. https://doi.org/10.1016/j.wear.2008.12.101
22. Moore MA (1974) The relationship between the abrasive wear resistance, hardness and microstructure of ferritic materials. Wear 28:59–68. https://doi.org/10.1016/0043-1648(74)90101-X
23. Arul Saravanapriyan SN, Vijayaraghavan L, Krishnamurthy R (2003) Significance of grinding burn on high speed steel tool performance. J Mater Process Technol 134:166–173. https://doi.org/10.1016/S0924-0136(02)00461-2